limited to simple commands such as "raise your hand". He failed even simple calculation (e.g. 1+2) both in oral and writing conditions. Indifference and lack of sympathy were noted as evidence of personality change. Mini-mental state examination scored 3/30, and he could not answer correctly even the first question of the Kohs block design test. A brain MRI demonstrated mild cortical atrophy with an ischemic lesion in the right parietal lobe. ^{123}I-IMP SPECT (N-isopropyl-p-[^{123}I] iodoamphetamine (IMP) single photon emission computed tomography) showed hypoperfusion in the bilateral frontal, temporal, and parietal lobes. An electroencephalogram showed frequent slow waves with irregular and unsteady alpha waves. The individual was tentatively diagnosed as having primary progressive aphasia.

At age 63, he was admitted to hospital to reevaluate his neurological condition. He still showed severe nonfluent aphasia. Although it was difficult to evaluate praxis and gnosia, no "alien hand" was observed. A neurologic examination revealed hyperreflexia in the all extremities, snout and sucking reflexes, as well as disorientation. No dysphagia was observed. He was still able to walk, dress, use chopsticks, and have a wash. He could still name real objects such as a pencil, scissors, wallet, ruler, and newspaper. Brain MRI demonstrated mild to moderate nonspecific cerebral cortical atrophy without significant laterality. The hippocampal formation as well as basal ganglia appeared to be normal in size. Periventricular hyperintensity of moderate degree suggestive of diffuse ischemia was present (Figure 1A–D). Based on the medical record of the outpatient clinic at age 63, pathologic reflexes and rigidity were recorded. L-DOPA had never been administered for his extrapyramidal symptoms. At age 64, he had an episode of pneumonia. Subsequently, he developed dysphagia, and because of subsequent walking disturbance he was limited to wheelchair conveyance. When he suffered from aspiration pneumonia at age 65, tracheotomy and percutaneous endoscopic gastrostomy (PEG) were carried out. He did not show any spontaneous speech. HMPAO-SPECT (99mTc-hexamethylpropyleneamine oxime single photon emission computed tomography) revealed diffuse cerebral hypoperfusion that was particularly prominent in the left frontal lobe. MRI showed severe cortical atrophy and enlargement of the lateral ventricles as well as dilatation of the central sulci and thinning of the corpus callosum. The left paracentral gyrus was significantly atrophic. The hippocampal formation also showed atrophy of moderate degree. The bilateral putamen was atrophic but with no signal alteration suggestive of increased iron deposition. Using fluid-attenuated inversion recovery (FLAIR) images, hyperintense lesions were shown in the cerebral white matter and hypointense lesions in the globus pallidus (Figure 1E–I). He died of aspiration pneumonia at age 67 and was tentatively diagnosed as having an atypical dementia. The patient's past medical history was acute hepatitis at age 30. Family history revealed that the patient's father died of cerebral infarction at age 92. However, no neurodegenerative diseases were recorded in the patient's family.

Macroscopic neuropathology

The harvested and fixed brain weighed 950 and 810 grams, respectively. A severe atrophy and an enlargement of the sulci were present at the frontal lobes (Figure 2A and B). The atrophy of the pars opercularis and enlargement of the central sulcus were prominent in the left hemisphere. The cerebral arteries showed moderate atherosclerotic changes. Coronal slices disclosed that cortical gray matter was much thinner than normal in the frontal cortex, and the lateral ventricles were enlarged. The anterior portion of the corpus callosum was atrophic. The head of the caudate nucleus and globus pallidus were moderately atrophic. Although the substantia nigra showed reduced pigmentation (Figure 2C), the color of the locus coeruleus was slightly reduced.

Microscopic neuropathology (Figures 2 and 3)

The neocortex showed severe neuronal cell loss and gliosis, with moderate to severe spongy state in the upper layers of the frontal and cingulate cortices. The frontal operculum was also severely affected. In the cerebral cortex, ischemic neurons were occasionally observed. In the fifth layer of the precentral cortex, the gliosis was more severe than in the other cortical layers. Severe neuronal loss and gliosis were seen in the globus pallidus interna (Figure 3A). Mild to moderate neuronal loss and gliosis were present in the claustrum, the head of caudate nucleus, putamen, globus pallidus externa, thalamus, and the amygdala. Ballooned neurons were numerous in the frontal and cingulate cortex, and occasionally seen in the temporal, parietal cortex as well as in the claustrum (Figure 2E). They were immunolabeled using antibody raised against neurofilament. In the hippocampus and parahippocampus, mild neuronal loss and gliosis as well as a few neurofibrillary tangles were present.

In the cerebellum, the dentate nucleus showed moderate neuronal loss and gliosis that were more severe in the right side. Grumose degeneration was

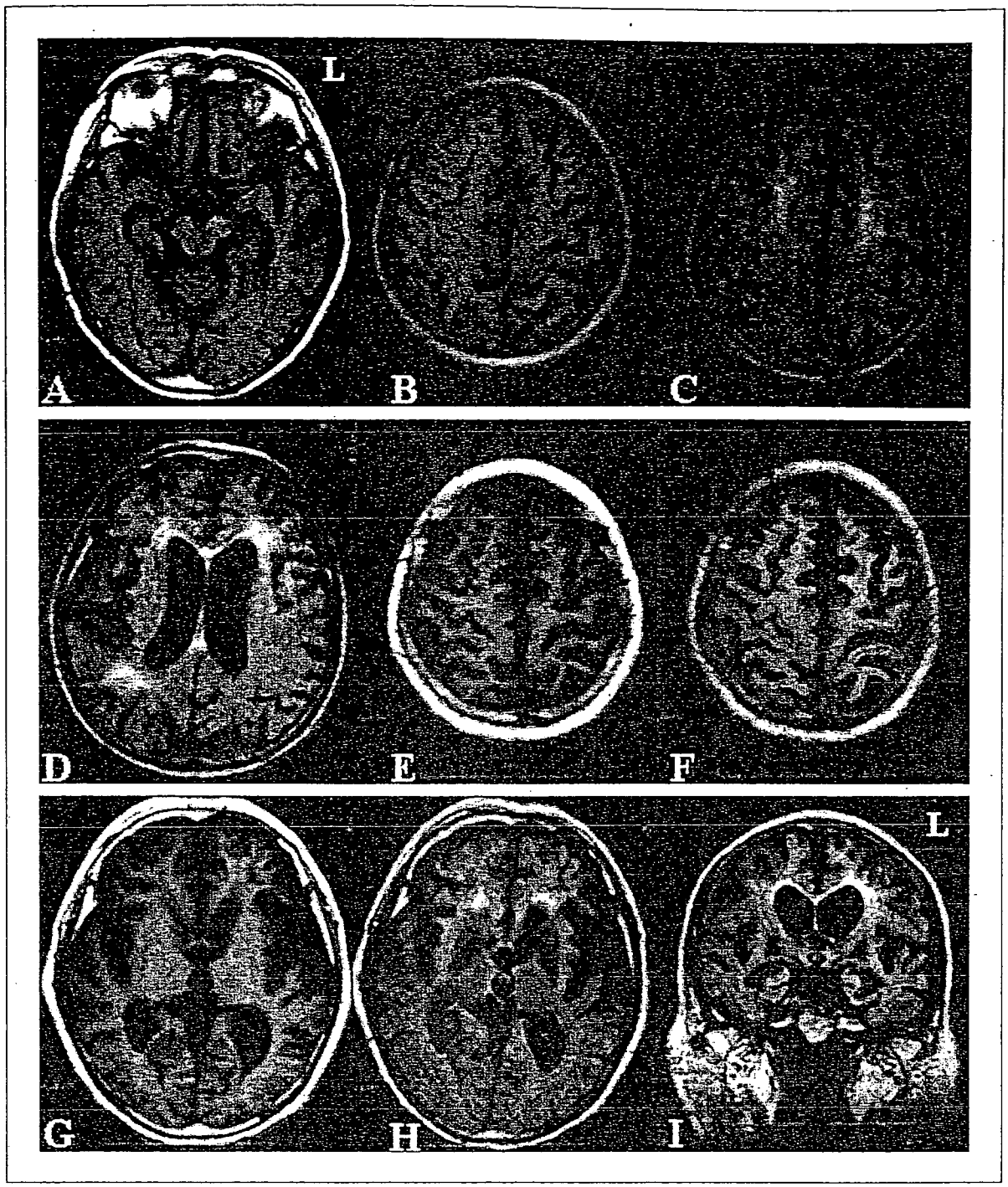

Figure 1. Magnetic resonance images taken at age 63 (A–D) and age 66 (E–I) show supratentorial ventricular dilation and prominent cortical sulci due to moderate to severe cortical atrophy. There is mild to moderate nonspecific cerebral cortical atrophy without significant laterality. The hippocampal formation as well as basal ganglia appears to be normal in size (A–C). Periventricular hyperintensity of moderate degree suggestive of diffuse ischemia was present (D). There is progressive mild atrophy in the paracentral cortex with predominance on the left side (B, C, E, F). The bilateral putamina are atrophic without signal decrease indicative of increased iron deposition (G, H). The hippocampal formation associated with dilatation of the inferior horn of the lateral ventricles is also noted (I). There are hypointense lesions at the level of the globus pallidus and hyperintense lesions in the cerebral white matter (I). (A, B, E, G: T1-weighted image (TR 440, TE 16); C, D, F, H, I: FLAIR (TR 8802, TE 112).)

also present in the neurons of the dentate nucleus. Although ischemic neurons were occasionally present in the Purkinje cell layer, the number of neurons in the cerebellar cortex was relatively well preserved. Severe neuronal loss and extra neuronal melanin deposits were observed in the substantia nigra (Figure 2D). Neuronal loss and gliosis were also present in the locus coeruleus. Neurofibrillary tangles were present in the periaqueductal gray matter, occulomotor nerve nucleus, substantia nigra, locus coeruleus, and raphe nucleus. The spheroids were occasionally observable in the substantia nigra. Frontopontine and pyramidal tracts showed mild loss of myelinated fibers suggesting mild degenerative condition.

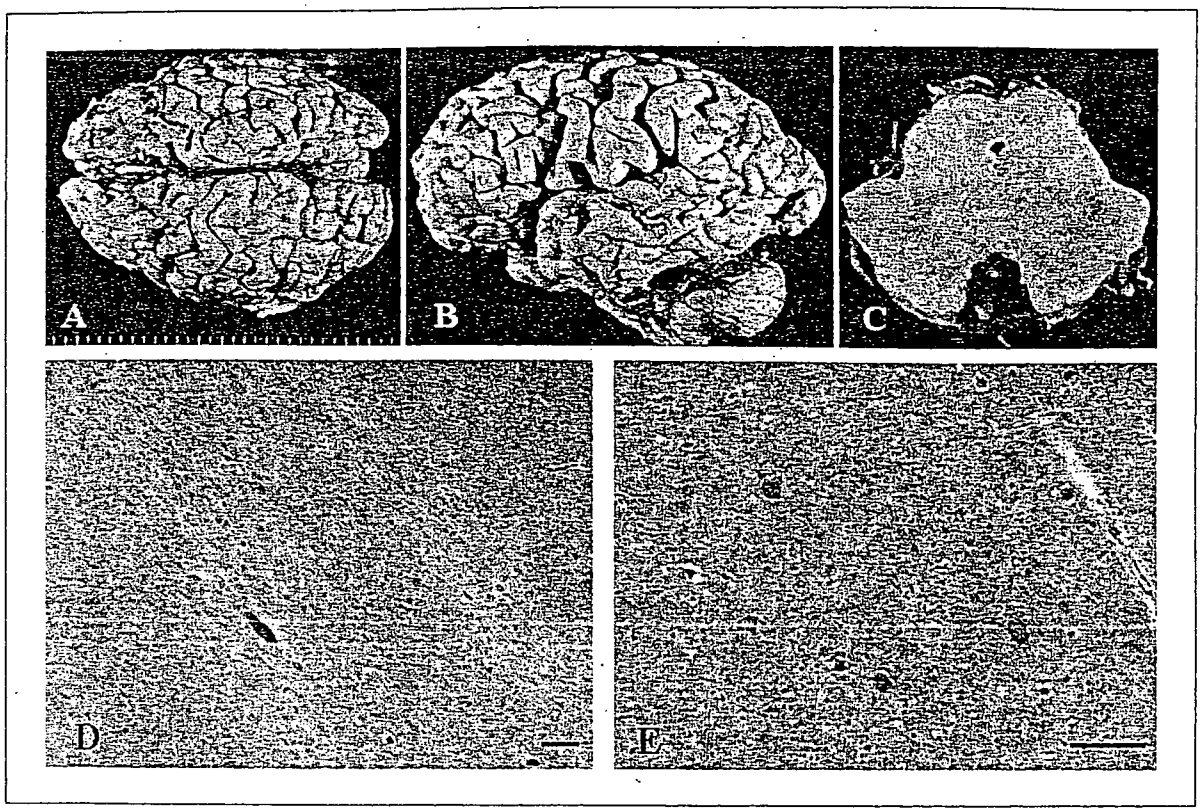

Figure 2. Macroscopic appearance of the proband's brain (A–C). Severe atrophy is present in the bilateral frontal lobes (A, B). Note the severe atrophy of the left operculum. Axial section of the midbrain shows severe depigmentation of the substantia nigra (C). Sections of the substantia nigra (D) and precentral gyrus (E). Severe neuronal loss and extraneuronal pigment are present in the substantia nigra (D). Numerous ballooned neurons are seen in the precentral cortex (E). (D, E: hematoxylin-eosin. Scale bars (D, E): 100 μm.)

Using a modified Gallyas-Braak method, various argentophilic deposits were seen in the neurons and glial cells (Figure 3B–N). In the cerebral cortex, numerous Gallyas-Braak-positive neurons were seen in the frontal, insular, parietal, and temporal cortex in which neuronal loss and gliosis were severe. Astrocytic plaques were also numerous in the frontal, temporal, and parietal cortex. In addition, Gallyas-Braak-positive neurons and astrocytic plaques were observed in the occipital cortex. The argentophilic threads were abundant in the frontal, temporal, parietal cortex as well as in the basal ganglia and brainstem nuclei. Numerous argentophilic threads were also seen in the white matter of the cerebrum, cerebellum and brainstem. There were no senile plaques, no Pick bodies or Lewy bodies in the cerebrum, cerebellum, and brainstem. An organizing infarct was present in the right parietal lobe in which the hyperintense ischemic lesion was observed using MRI (Figure 1).

Discussion

We describe a case of CBD with progressive nonfluent aphasia as an initial manifestation followed by dementia, parkinsonism, and pyramidal signs. Although the clinical appearance of the patient was unusual when compared with typical CBD, neuropathologic findings were consistent with the recent neuropathologic criteria of CBD *(9)*.

CBD is a relatively rare disorder and is clinically characterized by an akineto-rigid syndrome unresponsive to L-DOPA, with dystonic postures, apraxia, and a marked asymmetry of symptoms *(4,6,9)*. Recently, a similar clinical presentation was reported in an individual with progranulin gene mutation *(10)*. According to the analysis of 14 pathologically confirmed CBD cases, limb clumsiness and tremor were common symptoms followed by rigidity, apraxia, dystonia, and dementia *(7)*. Cognitive dysfunction of CBD has been considered as a rare or late manifestation *(4,7,11,12)*. In fact, one study showed that prominent sensory symptoms, isolated speech disturbance, and behavioral disturbance were rare initial presentations of CBD *(12)*. The diagnostic research criteria of CBD in 1994 mentioned that early dementia was an exclusion criteria for the diagnosis of CBD *(13)*.

As the number of autopsy-confirmed CBDs increased, cognitive impairment is now widely accepted as a common clinical feature *(4,6,9, 14,15)*. In fact, the present case showed difficulty in simple arithmetic calculation and dementia in early stage of clinical course. At this point, it is

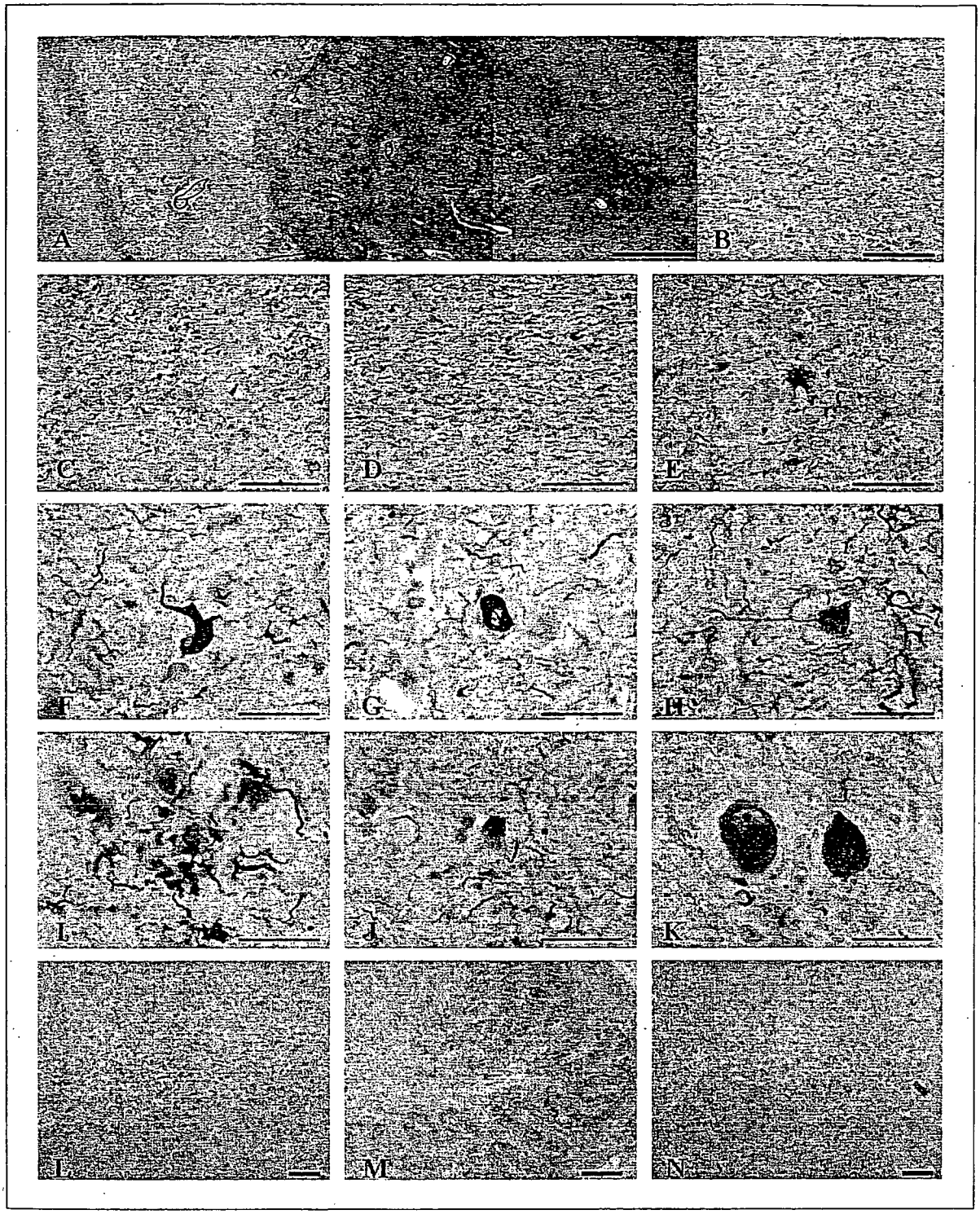

Figure 3. Macroscopic appearance of the basal ganglia (A). Severe gliosis is present in the globus pallidus. Note the gliosis is more prominent in the globus pallidus interna. Sections of the globus pallidus (B), superior frontal gyrus (C–J), substantia nigra (K), basis pontis (L), inferior olivary nucleus (M), and dentate nucleus of the cerebellum (N). Various argentophilic deposits (neurofibrillary tangles, argyrophilic threads, astrocytic plaques) are seen in the neurons and glial cells. (A: Holzer stain; B–N: modified Gallyas-Braak stain. Scale bars (A): 2 mm; (B, L, N) 100 μm; (C–K) 50 μm; (M) 0.5 mm.)

difficult to identify the regions responsible for the cognitive dysfunction. Particularly interesting is the fact that several types of aphasia have been reported in association with CBD *(4)*. However, only limited cases of pathologically confirmed CBD showed primary progressive aphasia as an initial presentation (Table 1) *(4,15–22)*. According to those reports, clinical heterogeneity of progressive aphasia was seen in the individuals with CBD. Unfortunately, we cannot clearly show the specific regions in association with progressive aphasia in the present case. Because the present individual had a 7-year clinical course, it was difficult to analyze clinicopathological correlations between the final pathologic changes and initial clinical symptoms. Functional images may ▶

Table 1. The previous reported cases of pathologically confirmed corticobasal degeneration associated with primary progressive aphasia.

Author (year) *(ref)*	Age at onset	Age at death	Handedness	Type of PPA	Other initial symptoms	Most affected cerebral area
Lippa et al. 1990 *(19)*	72	78	Right	Nonfluent	None	Left-parasylvian
Lippa et al. (1991) *(18)*	66	68	NA	Transcortical expressive		Left-SFG
Lang (1992) *(13)*	64	73	NA	NA	None	NA
Arima et al. (1991) *(16)*	64	73	Right	Amnestic	Dysarthria, hearing loss	Left-STG frontal operculum
Sakurai et al. (1996) *(21)*	64	72	Right	Amnestic	Hearing loss	Right-frontal
Ikeda et al. (1996) *(17)*	58	67	Right	Sensory aphasia	Hearing loss	Left-STG
Mimura et al. (2001) *(20)*	62	65	Right	Transcortical motor	None	Left-IFG frontal operculum
Ferrer et al. (2003) *(22)*	66	73	Right	NA	None	NA
Present case	60	67	Right	Nonfluent	Difficulty in calculation	Left-IFG frontal operculum

PPA = primary progressive aphasia; STG = superior temporal gyrus; SFG = superior frontal gyrus; IFG = inferior frontal gyrus; NA = not available.

help to identify the responsible anatomic area of progressive aphasia of CBD.

In general, most of the individuals with primary progressive aphasia may show nonfluent aphasia. The severe atrophy of the pars opercularis of the left inferior frontal gyrus can be associated with nonfluent aphasia in the present individual. Any neuropathologic basis of primary progressive aphasia remains uncertain. According to the many autopsy analyses of primary progressive aphasia, approximately 60% of patients showed nonspecific focal (or lobar) atrophy or dementia lacking distinctive histology, while 20% of patients showed Alzheimer's disease *(15)*. In the remaining 20% with primary progressive aphasia, Pick's disease and ubiquitin immunopositive inclusion disease were reported *(15)*. However, only a limited number of cases was pathologically confirmed as CBD that showed primary progressive aphasia *(3,7,8,12,23)*. We believe that the present case is important to understand the clinical heterogeneity of CBD.

Although pyramidal signs and symptoms are relatively common features in the individuals with CBD *(3,7,8,12,23)*, they have not been well analyzed *(3)*. The patient here described showed hyperreflexia in the extremities and pathologic reflexes in the latter half of the clinical course. Neuropathologically, there were the severe gliosis in the fifth layer of the motor cortex as well as pyramidal tract degeneration at the basis pontis and pyramids of the medulla oblongata. This finding strongly supports the recent findings of clinicopathologic correlation of pyramidal symptoms in CBD *(1,2,9,11)*.

The cortical atrophy, ballooned neurons, and degeneration of the substantia nigra have been emphasized as the neuropathologic features of CBD *(9)*. Recent neuropathologic criteria emphasize Gallyas-Braak-positive or tau-immunoreactive lesions in neurons, glia, and cell processes such as astrocytic plaques and thread-like lesions in both white matter and gray matter *(24)*. In the present case, astrocytic plaques were numerous and present along with neuronal loss in focal cortical regions. In addition, they were also seen in the occipital cortex. The severity and distribution of abnormal Gallyas-Braak-positive structures may be considerably different in each case of CBD. Systematic neuropathologic analysis of abnormal tau deposits is important in order to explain the clinical heterogeneity of CBD.

Information on MRI findings of CBD was limited. According to the recent literature, the most common findings are the prominent cortical atrophy in the paracentral parietal region and the superior frontal gyrus, corpus callosum atrophy, as well as the subcortical and periventricular white matter signal changes of MRI *(25,26)*. In the present case, the cortical atrophy was relatively diffuse and hippocampal formation was also atrophic. At the end of the clinical course, the proband's MRI showed hypointensity in the globus pallidus and hyperintensities in the cerebral white matter using FLAIR images. In addition, the bilateral putamen showed progressive atrophy. These changes were not seen in the MRIs carried out in the early stage of clinical course. The previous report showed that the hyperintense lesions of cerebral white matter might reflect demyelination *(27)*. In the present case, there were severe degeneration with argentophilic deposits and gliosis in the cerebral white matter. However, the hyperintense lesions of T2-weighted and FLAIR images in the subcortical area are occasionally present in healthy individuals *(28)*.

Further study may uncover the pathologic nature of the white matter lesions of corticobasal degeneration.

The T2-weighted signal hypointense lesion in the globus pallidus was observed in CBD *(29)*. The bilateral atrophy of the putamen was also reported in MRI. In a pathologic examination, the proband's brain showed severe degeneration of the globus pallidus. However, the interpretation of the MRI signal change of globus pallidus and atrophy of the putamen is difficult and must be cautious for the following reasons. First, the previous studies did not reveal any pathologic basis of the MRI changes in the basal ganglia. Second, the globus pallidus may show hypointensity using T2-weighted or FLAIR images even in normal individuals because of iron accumulation. Third, it was difficult to analyze the exact size of the putamen in this case by autopsy material. We believe that future analyses using MRI may enable investigators to reach increasingly accurate diagnoses of CBD.

We report an individual diagnosed with CBD who showed primary progressive aphasia. Neuropathologically, numerous argyrophilic structures, including astrocytic plaques, were observed in the neurons and glia. The pyramidal tract degeneration and loss of Bets cells were also present. This report will provide useful knowledge to understand the clinical heterogeneity of CBD. Better clinical and radiological criteria may ensure the accurate diagnosis of CBD.

Acknowledgements

This study was supported in part by Grants-in-Aid for Scientific Research (The Japan Society for the Promotion of Science 15600226).

REFERENCES

1. Rebeiz JJ, Kolodny EH, Richardson EP Jr. Corticodentatonigral degeneration with neuronal achromasia: a progressive disorder of late adult life. Trans Am Neurol Assoc. 1967;92:23–6.
2. Rebeiz JJ, Kolodny EH, Richardson EP Jr. Corticodentatonigral degeneration with neuronal achromasia. Arch Neurol. 1968;18:20–33.
3. Tsuchiya K, Murayama S, Mitani K, et al. Constant and severe involvement of Betz cells in corticobasal degeneration is not consistent with pyramidal signs: a clinicopathological study of ten autopsy cases. Acta Neuropathol (Berl). 2005;109:353–66.
4. Graham NL, Bak TH, Hodges JR. Corticobasal degeneration as a cognitive disorder. Mov Disord. 2003;18:1224–32.
5. Litvan I, Grimes DA, Lang AE, et al. Clinical features differentiating patients with postmortem confirmed progressive supranuclear palsy and corticobasal degeneration. J Neurol. 1999;246 Suppl 2:II1–5.
6. Mahapatra RK, Edwards MJ, Schott JM, Bhatia KP. Corticobasal degeneration. Lancet Neurol. 2004;3:736–43.
7. Wenning GK, Litvan I, Jankovic J, et al. Natural history and survival of 14 patients with corticobasal degeneration confirmed at postmortem examination. J Neurol Neurosurg Psychiatry. 1998;64:184-9.
8. Kompoliti K, Goetz CG, Boeve BF, et al. Clinical presentation and pharmacological therapy in corticobasal degeneration. Arch Neurol. 1998;55:957–61.
9. Dickson DW, Bergeron C, Chin SS, et al. Office of Rare Diseases neuropathologic criteria for corticobasal degeneration. J Neuropathol Exp Neurol. 2002;61:935–46.
10. Spina S, Murrell JR, Huey ED, et al. Corticobasal syndrome associated with the A9D Progranulin mutation. J Neuropathol Exp Neurol. In press.
11. Gibb WR, Luthert PJ, Marsden CD. Corticobasal degeneration. Brain. 1989;112:1171–92.
12. Rinne JO, Lee MS, Thompson PD, Marsden CD. Corticobasal degeneration. A clinical study of 36 cases. Brain. 1994;117:1183–96.
13. Lang AE, Riley DE, Bergerson C. Cortical-basal ganglionic degeneration. Philadelphia: WB Saunders; 1994.
14. Mesulam MM. Primary progressive aphasia. Ann Neurol. 2001;49:425–32.
15. Mesulam MM. Primary progressive aphasia—a language-based dementia. N Engl J Med. 2003;349:1535–42.
16. Arima K, Uesugi H, Fujita I, et al. Corticonigral degeneration with neuronal achromasia presenting with primary progressive aphasia: ultrastructural and immunocytochemical studies. J Neurol Sci. 1994;127:186–97.
17. Ikeda K, Akiyama H, Iritani S, et al. Corticobasal degeneration with primary progressive aphasia and accentuated cortical lesion in superior temporal gyrus: case report and review. Acta Neuropathol (Berl). 1996;92:534–9.
18. Lippa CF, Cohen R, Smith TW, Drachman DA. Primary progressive aphasia with focal neuronal achromasia. Neurology. 1991;41:882–6.
19. Lippa CF, Smith TW, Fontneau N. Corticonigral degeneration with neuronal achromasia. A clinicopathologic study of two cases. J Neurol Sci. 1990;98:301–10.
20. Mimura M, Oda T, Tsuchiya K, et al. Corticobasal degeneration presenting with nonfluent primary progressive aphasia: a clinicopathological study. J Neurol Sci. 2001;183:19–26.
21. Sakurai Y, Hashida H, Uesugi H, et al. A clinical profile of corticobasal degeneration presenting as primary progressive aphasia. Eur Neurol. 1996;36:134–7.
22. Ferrer I, Hernandez I, Boada M, et al. Primary progressive aphasia as the initial manifestation of corticobasal degeneration and unusual tauopathies. Acta Neuropathol (Berl). 2003;106:419–35.
23. Boeve BF, Maraganore DM, Parisi JE, et al. Pathologic heterogeneity in clinically diagnosed corticobasal degeneration. Neurology. 1999;53:795–800.
24. Valk J, Barkhof F, Scheltens P. Coricobasal degeneration. In: Valk J, Barkhof F, Scheltens P, editors. Magnetic resonance in dementia. Heidelberg: Springer-Verlag; 2002.
25. Hauser RA, Murtaugh FR, Akhter K, et al. Magnetic resonance imaging of corticobasal degeneration. J Neuroimaging. 1996;6:222–6.
26. Josephs KA, Tang-Wai DF, Edland SD, et al. Correlation between antemortem magnetic resonance imaging findings and pathologically confirmed corticobasal degeneration. Arch Neurol. 2004;61:1881–4.
27. Doi T, Iwasa K, Makifuchi T, Takamori M. White matter hyperintensities on MRI in a patient with corticobasal degeneration. Acta Neurol Scand. 1999;99:199–201.
28. Takao M, Koto A, Tanahashi N, et al. Pathologic findings of silent hyperintense white matter lesions on MRI. J Neurol Sci. 1999;167:127–31.
29. Tokumaru AM, O'Uchi T, Kuru Y, et al. Corticobasal degeneration: MR with histopathologic comparison. AJNR Am J Neuroradiol. 1996;17:1849–52.

EDITORIAL BOARD COMMENT

This case illustrates again that nonfluent primary progressive aphasia is a heterogeneous disorder with diseases like Alzheimer's, Creutzfeldt-Jakob disease, frontotemporal lobar degeneration (FTLD), progressive supranuclear palsy (PSP) as underlying cause. It again stresses the spectrum of so-called tauopathies to which most of these disorders belong.

complex cognitive tests and no significant changes on the repeated tests of simple reaction time. The second largest group of subjects were medicated with valproate (23%). Analysis of cognitive outcome of withdrawal of valproate revealed the same tendency as for the whole group and for carbamazepine but less clearly. The group of subjects on valproate was small, and there is therefore reason to be cautious about drawing conclusions on cognitive effects of this drug based on the present data.

The major finding in this study is that discontinuation of major AEDs significantly improves performance on tests that require complex cognitive processing under time pressure. The difference in speed of cognitive processing between the two groups on these tasks was between 24 to 43 milliseconds. Elements of these cognitive processes are necessary in many daily life activities and even a subtle slowing in processes that are repeated many times in daily life activities may have a significant impact. The results suggest that performance of certain kinds of intellectual work, tasks requiring divided attention, and fast information processing may be negatively affected by use of AEDs. Repeated testing of simple tasks of attention and reaction time revealed no significant differences between the withdrawal group and the non-withdrawal group. These results indicate that tasks requiring simpler forms of attention and simple reaction time are not significantly affected by major AEDs.

In conclusion, the major finding is that discontinuation of major AEDs in seizure-free patients significantly improves performance on tests that require divided attention and rapid information processing. The results suggest that seizure-free epilepsy patients can obtain improvement in cognitive function if they withdraw from antiepileptic treatment. All of the subjects in the study were on monotherapy, most of them with carbamazepine or valproate. The outcome of discontinuation of carbamazepine was similar to the outcome for the total study population, while withdrawal of valproate only revealed a non-significant tendency in the same direction. ■

REFERENCES

1. Vermeulen J, Aldenkamp AP. Cognitive side-effects of chronic antiepileptic drug treatment: a review of 25 years of research. Epilepsy Res. 1995;22:65–95.
2. Aldenkamp AP. Effects of Antiepileptic Drugs on Cognition. Epilepsia. 2001;42 Suppl 1:46–9.
3. Meador KJ. Cognitive effects of epilepsy and of antiepileptic medications. In: Wyllie E, editor. The treatment of epilepsy: principles and practice. 3rd ed. Philadelphia: Lippincott Williams & Wilkins; 2001. pp. 1215–1225.
4. Meador KJ. Cognitive and behavioural assessments in AED trials. Antiepileptic Drug Dev Adv Neurol. 1998;76:231–8.
5. Baker GA, Marson AG. Cognitive and behavioural assessments in clinical trials: what type of measure? Epilepsy Res. 2001;45:163–7.
6. Brunbech L, Sabers A. Effect of Antiepileptic Drugs on Cognitive Function in Individuals with Epilepsy. Drugs. 2002;62:593–604.
7. Cochrane HC, Anthony GM, Baker GA, et al. Neuropsychological outcomes in randomized controlled trials of antiepileptic drugs: a systematic review of methodology and reporting standards. Epilepsia. 1998;39:1088–97.
8. Miller EN. California Computerized Assessment Battery (CalCAP) Manual. Los Angeles: Norland Software; 1980.
9. Meador KJ, Loring DW, Allen ME, et al. Comparative cognitive effects of carbamazepine and phenytoin in healthy adults. Neurology. 1991;41:1537–40.
10. Gillham RA, Williams N, Wiedman K, et al. Concentration-effect relationships with carbamazepine and its epoxide on psychomotor and cognitive function in epileptic patients. J Neurol, Neurosurg Psychiatry. 1988;51:929–33.
11. Martin EM, Pitrak DL, Novak RM, et al. Reaction times are faster in HIV-seropositive patients on antiretroviral therapy: A preliminary report. J Clin Exp Neuropsychol. 1999;5:730–5.
12. Miller EN. Cognitive testing using reaction time and traditional neuropsychological procedures. J Int Neuropsychol Soc. 1995;1:393.
13. Miller EN, Satz P, Visscher B. Computerized neuropsychological assessment for HIV-related encephalopathy. Symposium on Novel and Traditional Approaches for Early Detection of HIV-1 Related Dementia (Vancouver, Canada). J Clin Exp Neuropsychol. 1989;11:34–5.
14. Miller EN, Satz P, Visscher B. Computerized and conventional neuropsychological assessment of HIV-1 infected homosexual men. Neurology. 1991;41:1608–16.
15. Worth JL, Savage CR, Baer L, et al. Computer-based neuropsychological screening for AIDS dementia complex. AIDS. 1993;7:677–81.
16. Miller EN. Use of computerized reaction time in the assessment of dementia (abstract). Neurology. 1992;42 suppl 3:220.
17. Lossius MI, Stavem K, Gjerstad L. Predictors for recurrence of epileptic seizures in a general epilepsy population. Seizure. 1999;8:476–9.
18. Kwan P, Brodie MJ. Early identification of refractory epilepsy. N Engl J Med. 2000;342:314–9.
19. Chen YJ, Chow JC, Lee IC. Comparison the cognitive effect of anti-epileptic drugs in seizure-free children with epilepsy before and after drug withdrawal. Epilepsy Res. 2001;44:65–70.
20. Aldenkamp AP, Alpherts WCJ, Blennow G, et al. Withdrawal of antiepileptic medication: effects on cognitive function in children: the results of the multicentre "Holmfrid" study. Neurology. 1993;43:41–51.
21. Meador KJ, Loring DW, Abney OL, et al. Effects of carbamazepine and phenytoin on EEG and memory in healthy adults. Epilepsia. 1993;34:153–7.
22. Meador K, Loring DW, Ray PG, et al. Differential cognitive and behavioural effects of carbamazepine and lamotrigine. Neurology. 2001;56:1177–82.
23. Thompson PJ, Huppert F, Trimble MR. Anticonvulsant drugs, cognitive function and memory. Acta Neurol Scand. 1980;S80:75–80.
24. Thompson PJ, Trimble MR. Sodium valproate and cognitive function in normal volunteers. Br J Clin Pharmacology. 1981;12:819–24.
25. Craig I, Tallis R. Impact of valproate and phenytoin on cognitive function in elderly patients. Results of a single blind randomised comparative study. Epilepsia. 1994;35:381–90.
26. Prevey ML, Delaney RC, Cramer JA, et al. Effect of valproate on cognitive function: comparison with carbamazepine: the Department of Veterans Affairs Epilepsy Cooperative Study 264 Group. Arch Neurol. 1996;53:1008–16.
27. Gallassi R, Morreale A, Di Sarro R, et al. Cognitive effects of antiepileptic drug discontinuation. Epilepsia. 1992;33:41–4.
28. Gillham RA, Read CL, McKee PJW, et al. Cognitive function in Adult Epileptic Patients on Long-Term Sodium Valproate. J Epilepsy. 1991;4:205–10.

EDITORIAL BOARD COMMENT

The present study confirms an improvement in certain cognitive functions after discontinuation of anti-epileptic drugs, such as carbamazepine and valproate. The improvement might be of relevance for the individuals in their daily life activities. Even though all included cases were below 67 years, it is reasonable to expect at least the same effects in elderly patients. The results bring attention to the importance of an evaluation of present medication and possible negative side effects as a part of the diagnostics of cognitive malfunctioning.

Use of scatter correction in quantitative I-123 MIBG Scintigraphy for differentiating patients with Parkinsonism: Results from Phantom experiment and Clinical Study

Bai J[1], Hashimoto J[2], Suzuki T[2], Nakahara T[2], Kubo A[2], Ohira M[3], Takao M[3], Ogawa K[4]

[1] 21st Century Center of Excellence Program, School of Medicine, Keio University, Tokyo
[2] Department of Radiology, School of Medicine, Keio University, Tokyo
[3] Department of Neurology, School of Medicine, Keio University, Tokyo
[4] Department of Electronic Informatics, Hosei University, Tokyo, Japan

Abstract

The aims of this study were to elucidate the feasibility of scatter correction in improving the quantitative accuracy of the Heart-to-Mediastinum (H/M) ratio in I-123 MIBG imaging and to clarify whether the H/M ratio calculated from the scatter corrected image improves the accuracy of differentiating patients with Parkinsonism from other neurological disorders. The H/M ratio was calculated using the counts from planar images processed with and without scatter correction in the phantom and on patients. The triple energy window (TEW) method was used for scatter correction. Fifty five patients were enrolled in the clinical study. The Receiver Operating Characteristic (ROC) Curve analysis was used to evaluate diagnostic performance. The H/M ratio was found to be increased after scatter correction in the phantom simulating normal cardiac uptake, while no changes were observed in the phantom simulating no uptake. It was observed that scatter correction stabilized the H/M ratio by eliminating the influence of scatter photons originating from the liver, especially in the condition of no cardiac uptake. Similarly, scatter correction increased the H/M ratio in conditions other than Parkinson's disease but did not show any change in Parkinson's disease itself to widen the differences in the H/M ratios between the two groups. The overall power of the test did not show any significant improvement after scatter correction in differentiating patients with Parkinsonism. Based on the results of this study it has been concluded that scatter correction improves the quantitative accuracy of H/M ratio in MIBG imaging, but it does not offer any significant incremental diagnostic value over conventional imaging (without scatter correction). Nevertheless it is felt that the scatter correction technique deserves special consideration in order to make the test more robust and obtain stable H/M ratios.

Key words: MIBG Imaging, Parkinson's disease, Parkinsonism, Scatter Correction, Triple Energy Window.

World J Nucl Med 2007;6:12-18

Introduction

Iodine 123 labeled Metaiodobenzylguanidine (I-123 MIBG), a norepinephrine analogue which is taken up and stored in the sympathetic nerve endings has been used to evaluate cardiac sympathetic nerve function (1). A number of investigators have reported the reduction in cardiac MIBG uptake in patients with Parkinson's disease (PD) and Dementia with Lewy Body (DLB) and its relative preservation in other neurological disorders like multiple system atrophy (MSA) and Cerebrovascular disease (CVD) (2-7). The authors of all the above cited reports have used quantitative methods to determine MIBG uptake in the determination of cardiac sympathetic nerve function. The index which has been most frequently used by most investigators is the heart to mediastinum (H/M) ratio that denotes the ratio of MIBG uptake in the myocardium over that in the mediastinum in an anterior planar image. The H/M ratio has proven to be very useful and shown relatively lower intra-subject variation (1). However, Nagayama and co-authors in a recently published study have reported considerable overlap in the values of H/M ratio between PD and non-PD patients (8), suggesting thereby the limitation of this parameter in differentiating patients with Parkinsonism from other neurological disorders. There are at least two conceivable reasons which could account for this overlap: 1. The real overlap of cardiac MIBG uptake values between the groups and 2. Technical error in calculating H/M ratios.

Correspondence:
Dr. Jingming Bai
21st Century Center of Excellence Program
School of Medicine
Keio University, Tokyo
Japan
E-mail: bjingming@goo.ne.jp

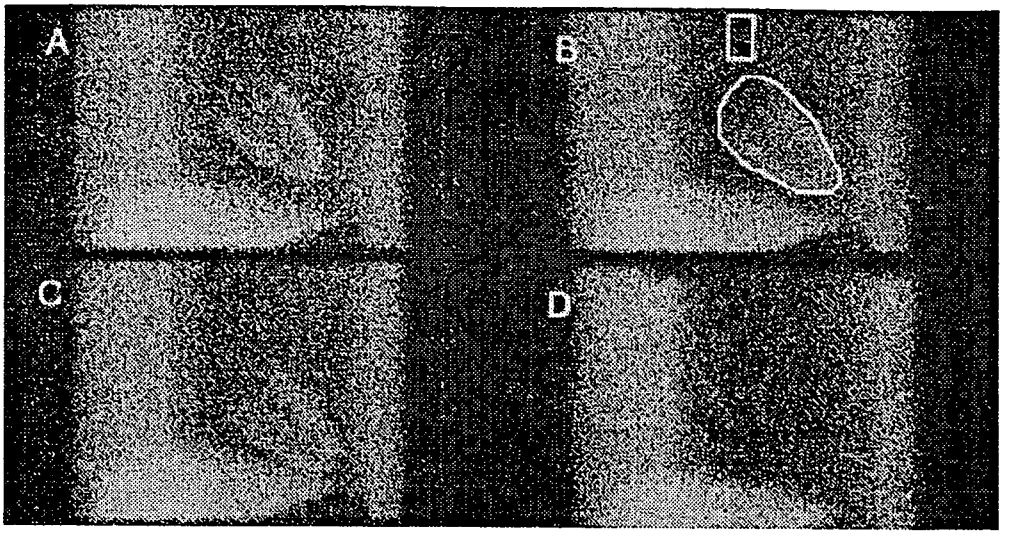

Figure 1. Configuration of the thoracic phantom. Panels A,B and C show the images obtained from the phantom containing the cardiac insert positioned far, normal (in between far and near) and near from liver, respectively. Panel D demonstrates the condition of no cardiac uptake. ROIs for heart and mediastinum are superimposed on the image of Panel B.

With regard to the technical aspects in the measurement, the problem caused by scattered photons in the region of interests (ROIs) is not negligible. This has been reported by several investigators (9-11). These reports have shown that reduction in the number of scattered photons by employing appropriate collimation and/or methods of scatter correction has improved the accuracy of H/M ratio in phantom experiments. In addition, clinically in patients suffering from cardiac diseases, scatter correction has been reported to increase the value of H/M ratio and decrease the variations caused by different collimations used (9). On the other hand, patients with PD often manifest no cardiac uptake of MIBG (3,5), and the effect of scatter reduction in images of such patients remains unclear. Nevertheless, there are few reports which have addressed the effect of correction in differentiating patients with Parkinsonism from other neurological disorders.

The aims of the present study were to elucidate the usefulness of scatter correction in the accurate quantification of the H/M ratio under different conditions of MIBG uptake and to clarify whether the H/M ratio obtained from scatter corrected images improves the accuracy of differentiating patients with Parkinsonism. We performed phantom experiments simulating patients with variable degrees of severity of nerve dysfunction and enrolled PD and non-PD patients in the clinical study.

Materials and Methods

A thoracic phantom (Kyoto-kagaku, Co., Kyoto, Japan) with a cardiac insert and the structures of mediastinum, lung, liver, stomach and vertebrae was used in this study (Figure 1). The cardiac insert consists of the left ventricular wall (120 ml), the left ventricular cavity (95 ml) and right ventricular cavity (105 ml). The compartmental volumes of the phantom were 2850 ml for the mediastinum including the cardiac insert, 710 ml for right lung, 540 ml for left lung, 1100 ml for liver and 290 ml for stomach. The distance between the cardiac insert and liver is adjustable.

Different radioactivity concentrations of I-123 MIBG (Daiichi Radioisotope Laboratories Ltd., Tokyo, Japan) were prepared for the left ventricular wall, liver, lung and mediastinum. The condition of normal cardiac nerve function was simulated by filling the left ventricular wall with 44.4 kBq/ml (1.2 μCi/ml) of I-123 MIBG, and the condition of no cardiac was simulated by removing the cardiac insert. Other concentrations were 29.6 kBq/ml (0.8 μCi/ml) for the liver, 23.7 kBq/ml (0.64 μCi/ml) for the lungs and 3.0 kBq/ml (0.08 μCi/ml) for the mediastinum. Thus the proportions of radioactive concentration in the heart, liver, lung and mediastinum were approximately 15:10:8:1 and 0:10:8:1 respectively corresponding to the conditions of simulated normal function and no cardiac uptake. The left and right ventricles and the stomach cavities were filled with water without radioactivity. Therefore the mean count per pixel in the liver ROI is higher than that in the cardiac ROI covering the whole heart, although radioactive concentration in the heart is 1.5 folds higher than that in the liver. On the setting of normal nerve function the position of the cardiac insert was changed to simulate the variations in the proximity of heart to the liver; e.g., very near, normal and away from the liver (Figure 1).

Clinical Study

Fifty-five patients, aged 63.0±14.7 years were included in the present study during the period from June 2004 to September 2005. The diagnosis of the clinical conditions is given in Table-1. The patients were divided into two categories: PD and non-PD categories. PD patients were diagnosed using the United Kingdom Parkinson's Disease

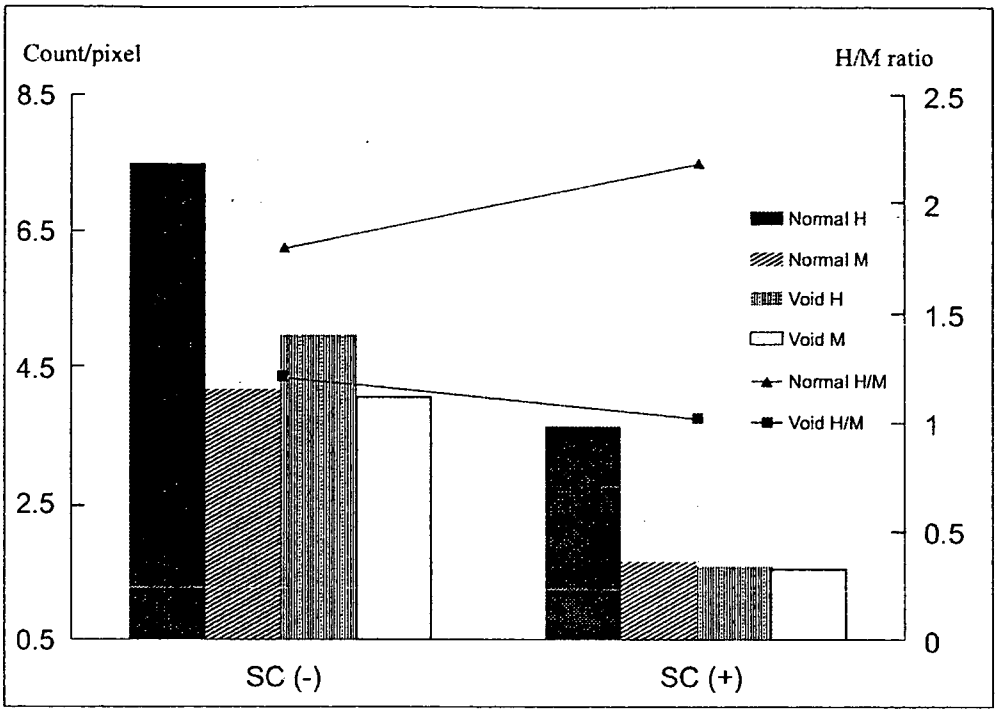

Figure 2. ROI counts and H/M ratios obtained with and without scatter correction. Bars represent the counts per pixel and the lines indicate the H/M ratios. Normal: Normal cardiac uptake; Void: No cardiac uptake; H: Heart; M: Mediastinum; H/M: heart-to-mediastinum count ratio; SC(-): without scatter correction; SC(+): With scatter correction.

Society Brain Bank Clinical Diagnosis Criteria (12,13). Individuals with the history of cardiac diseases or other factors possibly affecting sympathetic nerve function such as diabetes mellitus and antipsychotic drug administration were excluded. Informed consents were obtained from each patient before the examination. This study was conducted according to the Governmental and Institutional Regulations for protection of data privacy and confidentiality.

Data acquisition

Both in phantom as well as clinical studies, anterior planar images were obtained using a gamma camera system (GCA-9300A, Toshiba Corporation, Tokyo, Japan) equipped with a low energy, high resolution and parallel-hole collimator. According to the triple energy window (TEW) method (14,15), the acquisition windows used were as follows: 20% energy main window centered on the 159 keV photo-peak and two 7% sub-windows on both sides of the main window. Counts were acquired for 300 seconds on a 512x512 matrix. In the clinical study, images were acquired 3 hours after intravenous injection of 111 MBq (3 mCi) of I-123 MIBG.

Image Processing and Data Analysis

The data were processed with a medical image processor (GMS-5500A, Toshiba Corporation, Tokyo, Japan). Planar images with and without scatter correction were used for data analysis. In the TEW scatter correction method, the scatter fraction in the main window was estimated by the trapezoidal approximation based on first obtaining the counts in the sub-windows and then subtracting the same from the count in the main window to obtain a scatter-corrected image as in the previous studies (14,15). The order and cut-off frequency of the pre-filter for the sub-window were 8 and 0.07 (cycles/pixel), respectively. Filtering was not performed on the data of the main window. The selection of the filtering parameters was based on the results of our preparatory study performed prior to the present study (unpublished data). The image without scatter correction was generated only from the data in the main window.

A cardiac ROI was drawn manually over the contour of the heart and a rectangular mediastinal ROI was drawn in the upper mediastinum (Figure 1). The heart-to-mediastinum count ratios (H/M Ratios) were calculated from the mean counts per pixel in the ROIs over the heart and mediastinum before and after TEW correction.

Statistical Analyses

All the H/M ratios in the clinical study were expressed as Mean $\pm$ SD and were analyzed with Student's t test. Statistical significance was defined as $P<0.05$. The receiver operating characteristic (ROC) curve analysis was employed to evaluate the accuracy of differentiating PD patients from non-PD patients.

Results

Figure 2 shows the counts per pixel in the heart and mediastinal ROIs and the H/M ratios with and without scatter correction in the phantom study. In the phantom simulating normal function, the estimated H/M ratio

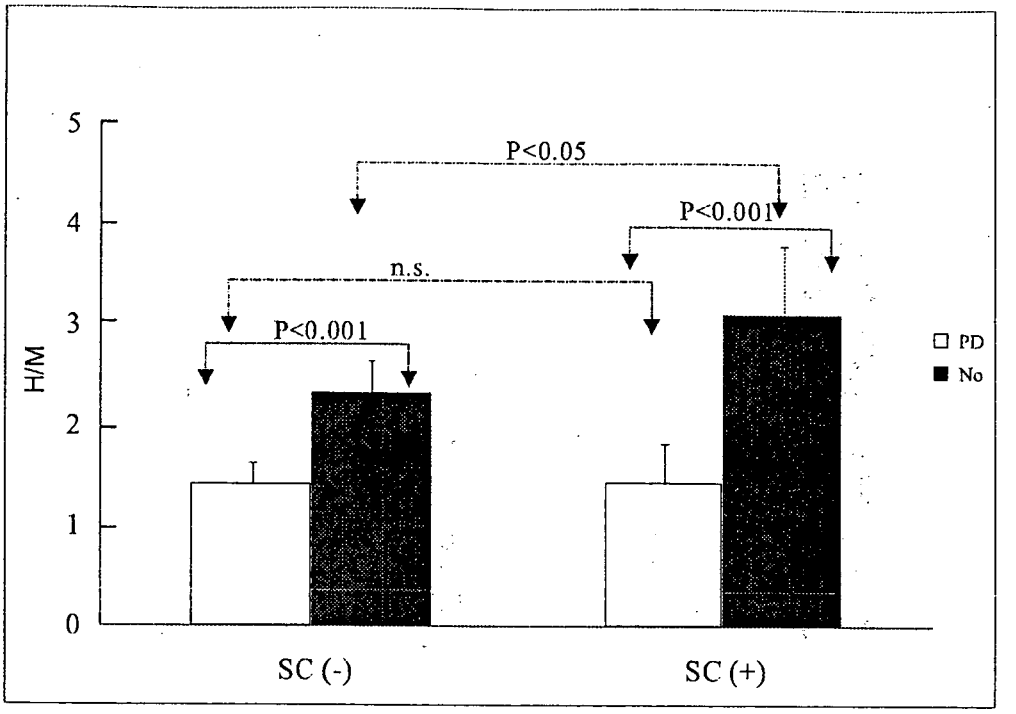

Figure 3. Comparison of H/M ratios (Mean ± SD) in patients with Parkinsonism in images processed with and without scatter correction. SC (-): without scatter correction; SC(+): With scatter correction; PD: Parkinson's Disease group; No: non-PD group

Group	Diagnosis	Number of cases
PD Group	Parkinson's Disease	21
	Dementia of Lewy Body	20
Non-PD Group	Multiple System Atrophy	34
	Dentatorubral-pallidoluysian Atrophy	1
	Cortico-basal Degeneration	01
	Amyotropic Lateral Sclerosis	02
	Alzheimer's Disease and Dementia	03
	Pure Akinesia	01
	Chronic Inflammatory Demyelinating Polyradiculoneuropathy	01
	Cerebrovascular Disease & Others	07
	Psychological Problems	02

Table 1. Patient population

	Near H/M	Far H/M	In between near and far
Normal Uptake			
SC(-)	1.94	1.91	1.02
SC(+)	2.39	2.33	1.03
No uptake			
SC(-)	1.44	1.35	1.07
SC(+)	1.24	1.25	0.99

Near H/M: H/M calculated keeping the distance between heart to liver ver near
Far H/M: H/M calculated keeping the distance between heart to liver far
SC(-): Without scatter correction
SC(+): With scatter correction

Table 2. Influence of Heart-to-Liver Distance on H/M Ratio

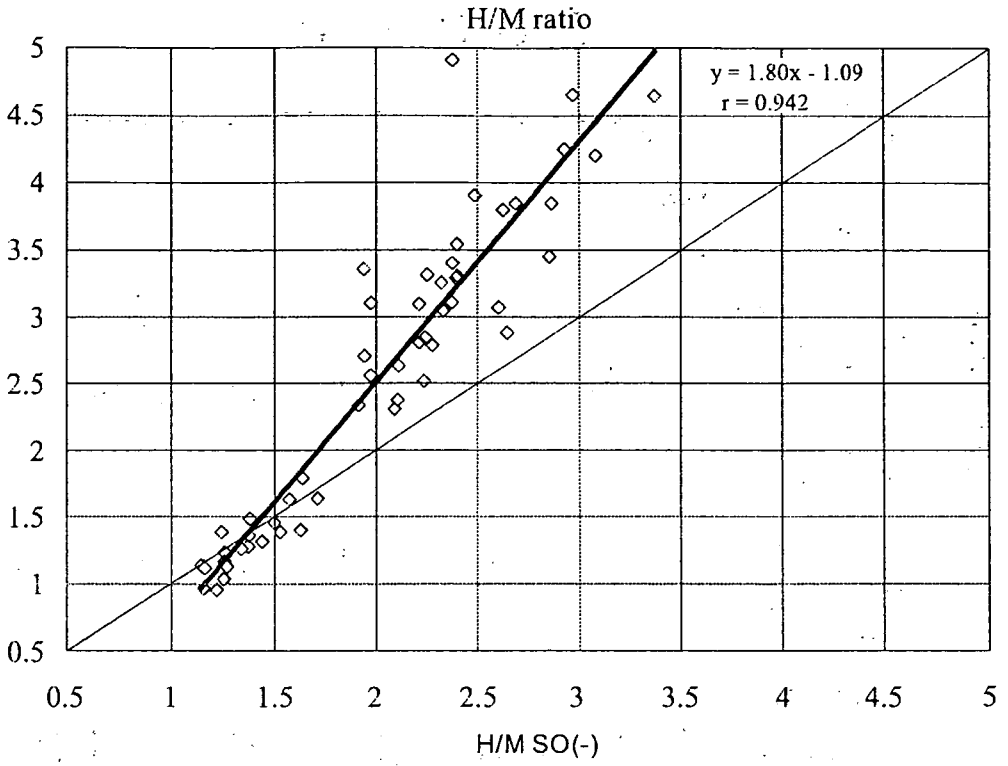

Figure 4. Relationship between H/M ratios with and without scatter correction. SC(-): without scatter correction; SC(+): With scatter correction; H/M SC(-): H/M ratio obtained without scatter correction; H/M SC(+): H/M ratio obtained with scatter correction.

increased after scatter correction. This is due to the more marked count reduction in the mediastinum compared to that in the heart. In contrast, in the phantom with no cardiac uptake, scatter correction produced a decreased H/M ratio by reducing the heart count much more than the mediastinal counts.

The influence of hepatic radioactivity on the H/M ratio was assessed by changing the distance between the heart and liver. The H/M ratio remained stable independent of the heart-to-liver distance in the phantom simulating normal function (Table 2); this stability was observed in the H/M values obtained from images with and without scatter correction. On the other hand, in the phantom simulating no cardiac output, the H/M ratio changed depending on the distance when not performing scatter correction and kept unchanged in the scatter corrected images, indicating that scatter correction could circumvent the distance-dependent variation of the H/M ratio.

Clinical Study

Figure 3 depicts the H/M ratios in PD and non-PD groups with and without scatter correction. Statistically significant difference was observed between the two groups both in scatter-corrected and uncorrected images. The H/M ratios showed no appreciable change after scatter correction in the PD group, while scatter correction yielded significantly increased H/M ratios in the non-PD group. Hence the differences were widened following scatter correction between the PD and non-PD groups.

Figure 4 illustrates the effect of scatter correction in each patient and relationship between H/M ratios with and without scatter correction. Increased H/M ratios after scatter correction were observed in patients with relatively well preserved MIBG uptake, whereas scatter correction resulted in decreased or unaltered H/M ratios in cases where the values were 1.5 or less.

The results of ROC analysis in separating PD and DLB from others are illustrated in figure 5. The areas under the curves were 0.961 and 0.941 in the diagnosis using uncorrected and scatter corrected H/M values, respectively. They were found to be statistically insignificant.

Discussion

Quantitative evaluation with the target-to-background count ratio is frequently used in routine scintigraphic studies because of its practicability. However, its accuracy is often degraded by scattered photons (15). With regard to the H/M ratio in I-123 MIBG imaging, scattered photons originating from the lungs contribute significantly to the mediastinal counts. In addition low cardiac uptake of MIBG may augment the influence of scattered photons from the liver to the heart ROI. Furthermore, the H/M ratio varies depending on the collimator selected and the variation is more remarkable when using low energy (LE) as compared with medium-energy (ME) collimators (10,11). The planar H/M ratios are less influenced by the septal penetration and scattered photons from liver activity when using medium-energy collimator (10). However, the

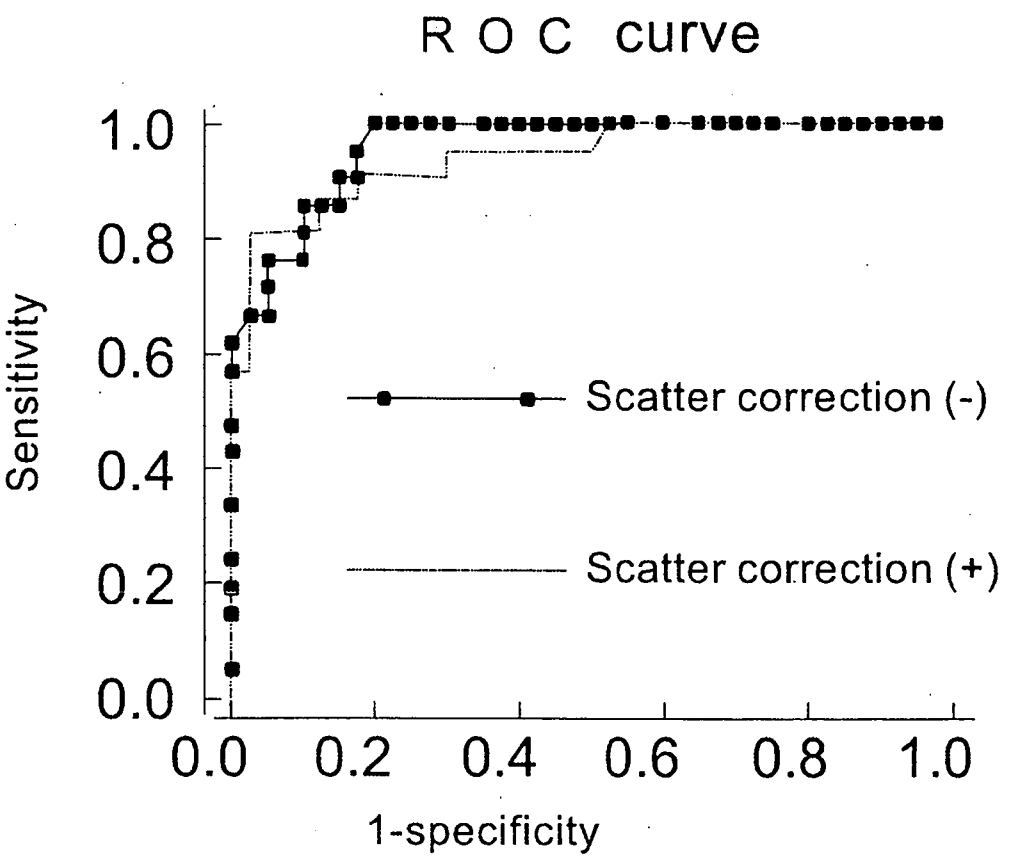

Figure 5. Accuracy of diagnosing Parkinson's disease using H/M ratios with and without scatter correction. Scatter correction (-): Without scatter correction; Scatter correction (+): With scatter correction.

low-energy collimator is still widely used in radionuclide imaging. Keeping in view the above practice, in the present study we implemented phantom as well as clinical imaging using the low-energy collimator under different grades of cardiac MIBG uptake in order to estimate the effect of scatter correction on quantification.

The results of the phantom experiment clarified the inherent inaccuracy of the H/M ratio. The H/M value was underestimated in the phantom simulating normal cardiac uptake and overestimated in the condition of severely decreased uptake. One of the reasons causing this error in estimation is photon scattering that could be overcome in clinical planar imaging.

The scatter fraction varies widely depending on the level of radioactivity in the target organ and adjacent tissues, and their anatomical relationship. In the condition of normal cardiac uptake, the scatter fraction in the heart ROI is smaller than that in the mediastinal ROI because the high cardiac count dominates scattered photons from adjacent organs resulting in an increase in the H/M value after scatter correction. In contrast, when cardiac uptake is severely reduced, the scatter fraction in the heart ROI is higher than that in the mediastinal ROI. This is due to the close proximity of liver to the heart ROI. In this case, the liver acts as the major source of scattered photons. Scatter correction decreases the H/M ratio in this condition. Hence, scatter correction may work to reduce the overlap of the H/M ratios among subjects with narrow differences of cardiac uptake. Moreover, scatter correction offers stable measurement of the H/M ratio regardless of the heart-to-liver distance by reducing the distance dependent effect of photon scattering (Table 2). This result demonstrates the usefulness of scatter correction in clinical practice in circumventing the inter-individual variations resulting from the difference of anatomical relationship between heart and liver.

A number of authors have reported the reduction of MIBG cardiac uptake in PD patients and not in non-PD patients (2,3,6). Meanwhile, the decrease of cardiac MIBG uptake in non-PD patients has also been reported, leading to overlap in H/M ratios obtained in PD and non-PD patients (8). None of the above articles employed scatter correction in calculating the H/M ratios. In the current study, scatter correction increased the H/M values in subjects with well-preserved cardiac sympathetic nerve function, while not in patients with severely impaired function (Figure 4). However ROC analysis revealed that scatter correction did not improve the diagnostic power (Figure 5). There are two possible reasons accounting for this result; number one reason being, that MIBG examination has inherently high diagnostic power regardless of the insufficient accuracy of the H/M index without scatter correction. This explanation is supported by the fact that the majority of papers in literature have reported acceptable diagnostic accuracy in differentiating PD from non-PD even without employing

scatter correction technique. The second reason could be that there are only a limited number of mild PD cases whose H/M values are in the border zone between PD and non-PD. There is a need for further studies including certain number of mild PD cases to clarify this aspect. Nevertheless on the basis of the present study and of several studies reported in literature it has been proven that conventional MIBG imaging can distinguish most of the patients with neurological disorders into PD and non-PD groups even without employing scatter correction.

Conclusions

Scatter correction was applied to MIBG planar images for calculating H/M ratios, and verified its feasibility through phantom and clinical studies. Scatter correction improved the separation of preserved cardiac uptake from reduced uptake, and stabilized the H/M calculations by reducing the influence of scatter photons from other adjacent organs. In differentiating patients with Parkinsonism, scatter correction did not offer any significant incremental diagnostic value to conventional images without scatter correction. Nevertheless the scatter correction method deserves consideration for use in calculating H/M ratio, because of its simplicity and effectiveness in eliminating the possible inaccuracies of the H/M ratio resulting from variations in the heart to liver distance.

Acknowledgement

This study was partially supported by the Ministry of Education, Culture, Sports, Science & Technology, Grant-in-aid for the 21st century Centre of Excellence (COE) program entitled, "Basic study and clinical application of human stem cell biology and immunology: Kyoto University, Japan

References

1. Somsen GA, Verberne HJ, Fleury E, Righetti A. Normal values and within-subject variability of cardiac I-123 MIBG scintigraphy in healthy individuals: Implications for clinical studies. J Nucl Cardiol 2004; 11: 126-133
2. Yoshita M. Differentiation of idiopathic Parkinson's disease from striatonigral degeneration and progressive supranuclear palsy using Iodine-123 MIBG myocardial scintigraphy. J Neurol Sci 1998; 155: 60-67.
3. Satoh A, Serita T, Seto M, et al. Loss of I-123 MIBG uptake by the heart in Parkinson's disease: Assessment of cardiac sympathetic denervation and diagnostic value. J Nucl Med 1999; 40: 371-375.
4. Orimo S, Ozawa E, Nakade S, Sugimoto T, Mizusawa H. I-123 MIBG myocardial scintigraphy in Parkinson's Disease. J Neurol Neurosurg Psychiatry 1999; 67: 189-194.
5. Courbon F, Brefel-Courbon C, Thalamas C, et al. Cardiac MIBG scintigraphy in a 'sensitive tool for detecting cardiac sympathetic denervation in Parkinson's Disease. Mov Disord 2003; 18: 890-897.
6. Orimo S, Amino T, Ozawa E, et al. A useful marker for differential diagnosis of Parkinson's Disease MIBG Myocardial scintigraphy. Rinsho Shinkeigaku 2004; 44: 827-829.
7. Lee PH, Kim JS, Shin DH, Yoon SN, Hul K. Cardiac I-123 MIBG Scintigraphy in patients with drug-induced Parkinsonism. J Neurol Neurosurg Psychiatry 2005; 77: 272-374.
8. Nagayama H, Hamamato M, Ueda M, Nagashima J, Katayama Y. Reliability of MIBG myocardial scintigraphy in the diagnosis of Parkinson's Disease. J Neurol Neurosurg Psychiatry 2005; 76: 249-251.
9. Kobayashi H, Momose M, Kanaya S, Kondo C, Kusakabe K, Mitsuhashi N. Scatter correction by two window standardized cardiac I-123 MIBG uptake in various gamma camera systems. Ann Nucl Med 2003; 17: 309-313.
10. Inoue Y, Suzuki A, Shirouzu I, et al. Effect of collimator choice on quantitative assessment of cardiac Iodine 123 MIBG uptake. J Nucl Cardiol 2003; 10: 623-632
11. Verberne HJ, Feenstra C, de Jong WM, Somsen GA, van Eck-Smit BL, Busemann Sokole E. Influence of collimator choice and simulated clinical conditions on I-123 MIBG Heart/Mediastinum ration: A Phantom Study. Eur J Nucl Med Mol Imaging 2005; 32: 1100-1107.
12. Gibb WK, Lees AJ. The relevance of the Lewy body to the pathogenesis of the idiopathic Parkinson's Disease. J Neurol Neurosurg Psychiatry 1988; 51: 745-752.
13. Hughes AJ, Daniel SE, Lees AJ. Improved accuracy of clinical diagnosis of Lewy Body Parkinson's Disease. Neurology 2001; 57: 1497-1499.
14. Ogawa K. Simulation study of triple-energy-window scatter correction in combined Tl-201, Tc-99m SPECT. Ann Nucl Med 1994; 8: 277-281.
15. Hashimoto J, Sasaki T, Ogawa K, et al. Effects of scatter and attenuation correction on quantitative analysis of a-CIT brain SPET. Nucl Med Commun 1999; 20: 159-165.

INTERNAL MEDICINE

□ PICTURES IN CLINICAL MEDICINE □

'Hot-cross Bun Sign' of Multiple System Atrophy

Masaki Takao[1], Taro Kadowaki[2], Yutaka Tomita[2], Yoji Yoshida[1] and Ban Mihara[2]

Key words: hot-cross bun sign, multiple system atrophy, MRI, neuropathology

(DOI: 10.2169/internalmedicine.46.0514)

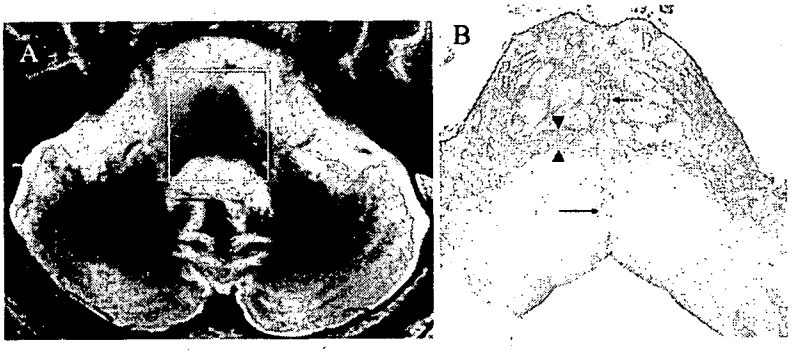

Picture 1.

Well known 'hot-cross bun sign' (cruciform hyperintensity, HCB) may be observed in patients with the cerebellar variant of multiple system atrophy (MSA-C) as well as SCA2 and SCA3 (1, 2). However, the radiological and neuropathologic correlation of HCB has not been well analyzed (1). A 43-year-old man developed dizziness followed by dysarthria, ataxia and Parkinsonism. He was diagnosed as having MSA-C and died of pneumonia at age 49. Postmortem 3.0T-MRI (GE Medical Systems Signa EXCITE) showed HCB at the level of pons on T2WI (TR4800, TE92) (Picture 1A). To clarify the pathologic basis of HCB, we prepared a histological section at the same plane of MRI (Box in Picture 1A). In addition to the loss of neurons and myelinated fibers at the basis pontis, the section of Holzer stain showed gliosis of the following three regions: 1) middle part of the reticular formation (arrow), 2) the pontocerebellar fiber between the medial lemniscus and pyramidal tract (arrowheads), and 3) the crossing part of the pontocerebellar fibers at the basis pontis (broken line arrow) (Picture 1B). Because astrocytosis increases the local water content (3), we believe that HCB primarily reflects the gliosis rather than only the loss of neurons. We also obtained similar results based on the analysis of a case of SCA2 (data not shown). Our approach may shed light on the study of the clinical-radiological-pathological correlation in neurological disorders.

References

1. Burk K, Skalej M, Dichgans J. Pontine MRI hyperintensities ("the cross sign") are not pathognomonic for multiple system atrophy (MSA). Mov Disord **16**: 535, 2001.
2. Murata Y, Yamaguchi S, Kawakami H, et al. Characteristic magnetic resonance imaging findings in Machado-Joseph disease. Arch Neurol **55**: 33-37, 1998.
3. Awad IA, Johnson PC, Spetzler RF, Hodak JA. Incidental subcortical lesions identified on magnetic resonance imaging in the elderly. II. Postmortem pathological correlations. Stroke **17**: 1090-1097, 1986.

[1]Department of Cognitive and Intractable Neurological Disorders, Mihara Memorial Hospital, Isesaki and [2]Department of Neurology, Mihara Memorial Hospital, Isesaki

Received for publication August 11, 2007; Accepted for publication August 30, 2007

Correspondence to Dr. Masaki Takao, takao-jscn@umin.ac.jp

 Journal Website: http://www.naika.or.jp/imindex.html

NEUROLOGY INDIA
Publication of the Neurological Society of India

NEUROIMAGE
Year : 2007 | **Volume** : 55 | **Issue** : 2 | **Page** : 186-

Brain magnetic resonance imaging unveils the history of carbon monoxide poisoning

***Takao* Masaki[1], *Mihara* Ban[2],**
[1] Department of Legal Medicine, School of Medicine, Keio University, Shinjuku-ku, Tokyo; Department of Neurology, Mihara Memori Hospital, Isesaki, Gunma, Japan
[2] Department of Neurology, Mihara Memorial Hospital, Isesaki, Gunma, Japan

Correspondence Address:
Takao Masaki
Department of Legal Medicine, School of Medicine, Keio University, Shinjuku-ku, Tokyo; Department of Neurology, Mihara Memorial Hospital, Isesaki, Gunma
Japan

How to cite this article:
Takao M, Mihara B. Brain magnetic resonance imaging unveils the history of carbon monoxide poisoning.Neurol India 2007;55:186-186

How to cite this URL:
Takao M, Mihara B. Brain magnetic resonance imaging unveils the history of carbon monoxide poisoning. Neurol India [serial online] 2007 [cited 2008 Feb 3];55:186-186
Available from: http://www.neurologyindia.com/text.asp?2007/55/2/186/32808

Full Text

A 64-year-old woman was referred to our hospital because of possible viral meningo-encephalitis. Two weeks prior to admission she developed a gait disturbance followed by a fever and headache. Neurological examination showed a small steppage gait, bradykinesia, and rigidity without tremor. However, deep tendon reflexes and cognitive function were normal. Cerebrospinal fluid was normal. A test using a nasopharyngeal swab indicated active infection of influenza A virus, prompting the introduction of oseltamivir that is anti-influenzaviral drug. Magnetic resonance imaging (MRI) using T2WI showed elliptical and diffuse hyperintense lesions in the bilateral globus pallidi [Figure 1]A and cerebral white matter [Figure 1]B, respectively. The lesions in the globus pallidi revealed irregular hyperintensity using T1WI. A detailed interview with her disclosed that she had accidentally inhaled carbon monoxide inhalation by an oil heater four weeks earlier.

Discussion

CO is a well-known toxic substance that has high affinity for hemoglobin. Neuropathologic alterations of CC intoxication are characterized by hemorrhagic necrosis of the globus pallidus and demyelination of the cerebral white matter.[1] Except for acute fatal cases, individuals who recover from acute exposure of CO

may develop a delayed neurological syndrome for up to 5 weeks after inhalation.[2],[3] In some instances, it may be difficult to diagnose accurately this delayed neurological syndrome because clinical settings compromise the gathering of medical histories of patients. In as much as she completely recovered from th acute manifestations of the exposure, her parkinsonism was not considered in association with carbon monoxide. This case came as a fresh reminder of the worth of MRI and the presence of delayed neurologic sequela of carbon monoxide poisoning.

References

1 Prockop LD, Naidu KA. Brain CT and MRI findings after carbon monoxide toxicity. J Neuroimaging 1999;9:175-81.

2 Kim JH, Chang KH, Song IC, Kim KH, Kwon BJ, Kim HC, *et al* . Delayed encephalopathy of acute carbon monoxide intoxication: Diffusivity of cerebral white matter lesions. AJNR Am J Neuroradiol 2003;24:1592-7.

3 Myers RA, Snyder SK, Emhoff TA. Subacute sequelae of carbon monoxide poisoning. Ann Emerg Med 1985;14:1163-7.

Original Research Article

Dementia and Geriatric Cognitive Disorders

Dement Geriatr Cogn Disord 2007;24:42–47
DOI: 10.1159/000102596

Accepted: March 9, 2007
Published online: May 10, 2007

Frequency and Clinical Characteristics of Early-Onset Dementia in Consecutive Patients in a Memory Clinic

Shunichiro Shinagawa[a, b] Manabu Ikeda[a, c] Yasutaka Toyota[a]
Teruhisa Matsumoto[a] Naomi Matsumoto[a] Takaaki Mori[a] Tomohisa Ishikawa[a]
Ryuji Fukuhara[a] Kenjiro Komori[a] Kazuhiko Hokoishi[a] Hirotaka Tanabe[a]

[a]Department of Neuropsychiatry, Neuroscience, Ehime University, Graduate School of Medicine, Ehime, [b]Department of Psychiatry, Jikei University School of Medicine, Tokyo, and [c]Department of Psychiatry and Neuropathobiology, Faculty of Medical and Pharmaceutical Science, Kumamoto University, Kumamoto, Japan

Key Words
Early-onset dementia · Alzheimer's disease · Frontotemporal lobar degeneration · Dementia with Lewy bodies · Memory clinic

Abstract
Aims: To investigate the frequency, rate of causes of dementia, and clinical characteristics of early-onset dementia in consecutive patients of a memory clinic. ***Methods:*** A total of 668 consecutive demented patients were involved in this study. We examined the distribution of patients' diagnosis, differences in sex, education, dementia severity and cognitive function at the first visit, and the duration from onset to consultation. We also examined the changes in the proportion of subjects during the research period. ***Results:*** There were 185 early-onset patients, 28% of all demented patients. No significant differences were observed between the early-onset and late-onset dementia groups in Clinical Dementia Rating and Mini-Mental State Examination score at the first consultation, but the duration from onset to consultation was significantly longer in the early-onset group. In the early-onset group, the rates of patients with Alzheimer's disease and dementia with Lewy bodies were relatively low and the rate of patients with frontotemporal lobar degeneration was relatively high. There were no significant differences in the proportion between either demented subjects and nondemented subjects or early-onset dementia patients and late-onset dementia patients during the research period. ***Conclusion:*** We conclude that early-onset dementia is not rare and its clinical characteristics and causes are different from late-onset dementia.

Introduction

Early-onset dementia (EOD), with onset in those younger than 65 years, has a large psychological and economical impact on patients and caregivers because of their leading role in the society and family at the disease onset. However, EOD has been underrecognized until today and social support services for EOD patients are not enough compared with those for late-onset dementia (LOD) patients.

Although there are some studies about early-onset Alzheimer's disease (AD) [1–3], there are few systematic studies about cognitive function in and clinical features of EOD of the non-Alzheimer type [4, 5]. Further, epidemiologic data on relatively rare causes of dementia, in-

KARGER
Fax +41 61 306 12 34
E-Mail karger@karger.ch
www.karger.com

1420–8008/07/0241–0042$23.50/0

Accessible online at:
www.karger.com/dem

Manabu Ikeda, MD PhD
Department of Psychiatry and Neuropathobiology
Faculty of Medical and Pharmaceutical Sciences, Kumamoto University
1-1-1, Honjo, Kumamoto 860-8556 (Japan)
Tel. +81 96 373 5184, Fax +81 96 373 5186, E-Mail mikeda@kumamoto-u.ac.jp

Table 1. Clinical characteristics of EOD patients and LOD patients

	EOD patients (n = 185; 27.7%)	LOD patients (n = 483; 72.3%)	p
Age at consultation, years	58.3 ± 11.0	77.9 ± 5.6	
Sex ratio (M:F)	94:91	188:295	0.007
Education[1], years	11.4 ± 2.8	9.5 ± 2.5	0.000
MMSE score at first consultation[2]	18.4 ± 7.8	18.4 ± 6.4	0.978
CDR at first consultation (0.5:1:2:3)[3]	50:50:53:12	108:167:148:34	0.326
Duration from onset to consultation, months	59.6 ± 70.8	35.7 ± 25.9	0.000

Those who could not undergo MMSE or CDR at their first consultation or whose caregivers' information on patients' education was inaccurate were excluded.
[1] n = 628.
[2] n = 637.
[3] n = 622.

cluding dementia with Lewy bodies (DLB) and frontotemporal lobar degeneration (FTLD), are insufficient because pure cross-sectional or population studies are impractical for rare diseases [6]. Therefore, we aimed to clarify the frequency of EOD, rate of causes of dementia, and clinical characteristics of EOD in consecutive patients of our memory clinic.

Method

A total of 861 consecutive patients visiting the Higher Brain Function Clinic of the Department of Neuropsychiatry, Ehime University Hospital between January 1997 and September 2005 were examined. Of the 861 patients assessed, more than 80% resided in the Ehime prefecture, within a 100-km radius of the hospital, at their first consultation. The Ehime prefecture is a rural area of Japan with 1.5 million people, 21% of whom are over 65 years old. Our clinic is one of the few specialized clinics for demented people where we can evaluate patients with brain MRI and HMPAO-SPECT. More than 40% of all patients were referred from other doctors. Fifty percent of referrals were received from psychiatrists who are experts in demented patients to some degree, and the others were received from general physicians and geriatricians.

All patients were seen by senior neuropsychiatrists and underwent physical and neurological examinations. Thirty-three patients who came to our clinic only once or who could not undergo neuroimaging examination were excluded, as they could not complete enough evaluations for us to make a clear diagnosis. Patients were assessed with a comprehensive neuropsychological test battery, which included the Mini-Mental State Examination (MMSE) [7], Clinical Dementia Rating (CDR) [8], together with standard psychiatric evaluations to exclude major functional psychiatric disorders such as schizophrenia and mood disorders. All patients underwent brain MRI, except those with cardiac pacemakers who underwent brain CT instead. Almost all patients underwent HMPAO-SPECT except those who could not because of their behavioral symptoms. Patients were also assessed with screening blood tests including vitamin B_{12}, folic acid and thyroid function.

Dementia was diagnosed according to the *Diagnostic and Statistical Manual of Mental Disorders*, 3rd edition revised [9]. Patients with AD satisfied probable AD criteria developed by the National Institute of Neurological and Communicative Disorders and Stroke and the Alzheimer's Disease and Related Disorders Association [10], and patients with vascular dementia (VaD) satisfied the criteria of the National Institute of Neurological Disorders and Stroke and the Association Internationale pour la Recherche et l'Enseignement en Neurosciences (NINDS-AIREN) [11]. DLB was defined according to the consensus guidelines for the clinical diagnosis of DLB [12]; FTLD was diagnosed according to the international consensus criteria [13]. Standard diagnostic criteria were also applied to dementia of other etiologies.

Information about onset of dementia was routinely and systematically queried from caregivers, and it was emphasized that 'onset' is the time when caregivers first noticed changes from the patients' premorbid state which should be substantive and not a long-standing character trait. One hundred and sixty patients were excluded as they did not fulfill the diagnostic criteria for dementia; 668 patients were included in this study. Among these nondemented patients, there were 31 patients with schizophrenia or delusional disorder, 19 patients with depression or anxiety disorder and 17 normal healthy subjects. The distribution of patients' diagnosis, differences in sex, educational level, severity of dementia according to CDR at the first visit, cognitive function according to MMSE at the first visit, and the duration from onset to consultation were compared between the EOD group (onset before the age of 65 years) and LOD group (onset after the age of 65 years). We examined the distribution of onset age and sex according to the causes of dementia in EOD patients. We also examined the changes in the proportion of subjects during the research period.

Data analyses were carried out using the SPSS-PC software package. Statistical differences between the EOD group and LOD group were assessed by the t test for age, education, duration from onset to consultation and MMSE score, and by the χ^2 test with post hoc Fisher's exact test for sex, CDR, distribution of diagnosis, and proportion of subjects. All examinations were conducted after obtaining informed consent from all subjects or their caregivers.

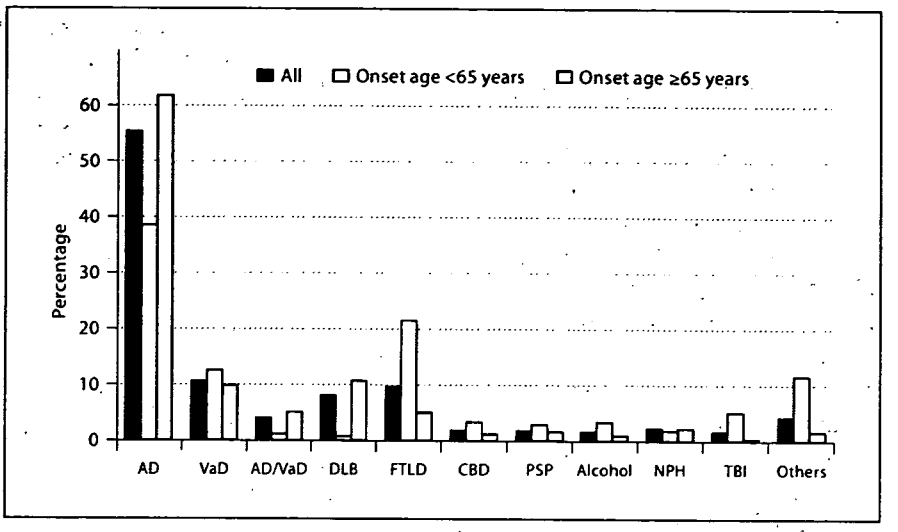

Fig. 1. Rate of causes of dementia in all patients, EOD patients and LOD patients. CBD = Corticobasal degeneration; PSP = progressive supranuclear palsy; alcohol = alcohol-related dementia; NPH = normal pressure hydrocephalus; others = dementia of other etiologies.

Result

Table 1 shows the clinical characteristics of the total 668 patients with dementia, comparing the EOD group and LOD group.

There were 185 EOD patients, 27.7% of all demented patients. In these EOD patients, mean age at consultation was 58.3 years and the sex ratio was almost equal (M:F = 94:91), meaning there were significantly fewer females than in the LOD group. Educational level was significantly higher than in LOD patients. There were no significant differences between the two groups in CDR and MMSE score at the first visit, but duration from disease onset to consultation was significantly longer in the EOD group compared to the LOD group.

Figure 1 shows the rate of causes of dementia in all patients, EOD and LOD groups.

Among all demented patients, AD was the most frequent cause of dementia (55.4%), followed by VaD (10.5%), FTLD (9.4%) and DLB (8.1%). Among EOD patients, AD was also the most frequent cause of dementia (38.5%). FTLD was the second most common cause of dementia (21.4%), followed by VaD (12.6%) and traumatic brain injury (TBI) (4.9%), and there were only a few DLB patients (0.5%). There were statistically significant differences between the EOD and LOD groups in the frequency of AD ($p = 0.000$), DLB ($p = 0.000$), FTLD ($p = 0.000$), alcohol-related dementia ($p = 0.031$), and TBI ($p = 0.000$). Neurosyphilis, carbon monoxide intoxication and post-encephalitis were relatively common in EOD patients with other etiologies.

Table 2. Changes in the proportion of subjects during the research period

	Demented		Nondemented	Total
	EOD	LOD		
1997–1999	39	146	56	241
2000–2002	69	164	63	296
2003–2005 (Sept.)	77	173	74	324
Total	185	483	193	861

Among all EOD patients and early-onset AD patients, the number of patients increased as the onset age got older, and there were no large differences in sex distribution in any generation. Among early-onset VaD patients, the number of patients increased with increasing onset age, and there were more males. Among early-onset FTLD patients, the number of patients increased after the age of 45 years, but no constant tendency was found in the sex ratio.

The changes in the proportion of subjects during the three sequential research periods are summarized in table 2.

Although the number of subjects increased with the passage of time in all groups, there were no significant differences in the proportion between either demented subjects and nondemented subjects or EOD patients and LOD patients. Among the demented patients, the severity of dementia according to CDR at the first consultation did not differ during the research period.